

See discussions, stats, and author profiles for this publication at: <https://www.researchgate.net/publication/278668883>

# Phase Change Characteristics in GeTe–CuTe Pseudobinary Alloy Films

ARTICLE *in* THE JOURNAL OF PHYSICAL CHEMISTRY C · NOVEMBER 2014

Impact Factor: 4.77 · DOI: 10.1021/jp5066264

---

CITATION

1

---

READS

13

3 AUTHORS, INCLUDING:



Yuta Saito

National Institute of Advanced Industrial Scie...

27 PUBLICATIONS 79 CITATIONS

SEE PROFILE



Junichi Koike

Tohoku University

178 PUBLICATIONS 3,559 CITATIONS

SEE PROFILE

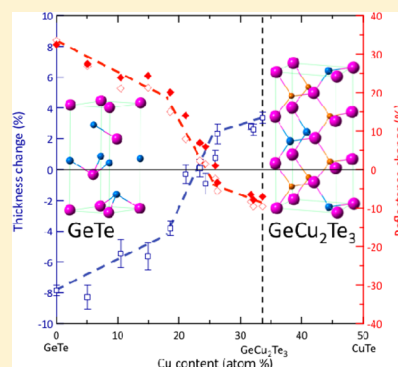
# Phase Change Characteristics in GeTe–CuTe Pseudobinary Alloy Films

Yuta Saito,<sup>\*,†</sup> Yuji Sutou,<sup>\*,‡</sup> and Junichi Koike<sup>§</sup>

<sup>†</sup>Nanoelectronics Research Institute, National Institute of Advanced Industrial Science & Technology (AIST), Tsukuba Central 4, Higashi 1-1-1, Tsukuba, Ibaraki 305-8562, Japan

<sup>‡</sup>Department of Materials Science, Graduate School of Engineering and <sup>§</sup>New Industry Creation Hatchery Center, Tohoku University, 6-6-11, Aoba-yama, Aoba-ku, Sendai 980-8579, Japan

**ABSTRACT:** Phase change characteristics in GeTe–CuTe pseudobinary alloy films, including GeCu<sub>2</sub>Te<sub>3</sub> (GCT), were investigated. The crystallization temperature of the amorphous film increased with increasing Cu content and then decreased again with further increasing Cu content. X-ray diffraction measurements revealed that the amorphous films with a composition range from 0 to 18.6 atom % Cu crystallized to GeTe single-phase, while the amorphous films with a composition range from 26.2 to 37.9 atom % Cu crystallized to GCT single-phase. The amorphous films with a composition between 21.1 and 24.3 atom % Cu showed a clear two-step crystallization during heating and finally formed the GeTe and GCT mixed-phase. The amount of volume shrinkage upon crystallization of the amorphous film decreased with increasing Cu contents, and the film with around 23 atom % Cu showed almost no volume change after crystallization. Meanwhile, film with over 25 atom % Cu showed volume expansion. It was found that no volume change was achieved by a two-step crystallization, namely, initial crystallization to GCT (volume expansion) with subsequent crystallization to GeTe (volume shrinkage). The film with no volume change also showed no reflectance change upon crystallization. The obtained results suggest that nonstoichiometric Ge<sub>50–x</sub>Cu<sub>x</sub>Te<sub>50</sub> films such as 26.2Cu film showing a small volume change without phase separation are preferable in terms of cyclability of phase change random access memory.



## INTRODUCTION

Phase change materials (PCMs) have been used for optical discs as well as for phase change random access memory (PCRAM).<sup>1</sup> In optical discs, the difference in reflectivity between amorphous and crystalline phases is used to store data and a laser pulse is applied to write and read the data. In PCRAM, the data is recorded by the difference in electrical resistivity of each phase and an electrical pulse is applied for data writing and reading. Ge<sub>2</sub>Sb<sub>2</sub>Te<sub>5</sub> (GST) has been extensively studied as a PCM of optical discs<sup>2</sup> and PCRAM<sup>3</sup> due to its fast crystallization and good repeatability. However, GST shows poor thermal stability because of its low crystallization temperature, and consequently, it is unsuitable for high temperature applications. Therefore, development of PCMs with a higher thermal stability than GST is desired.

Recently, Sutou and co-workers have proposed GeCu<sub>2</sub>Te<sub>3</sub> (GCT) compound for PCRAM material with a high thermal stability.<sup>4,5</sup> GCT film was found to show lower power consumption for amorphization than GST film and a fast crystallization regardless of having higher thermal stability.<sup>6,7</sup> Moreover, it is noteworthy that GCT amorphous film shows the volume expansion (+4%) and decrease in reflectance upon crystallization.<sup>7</sup> These unique features of GCT have been shown by theoretical calculations of the atomic structure together with the electronic structure.<sup>8</sup> Such unusual volume change upon crystallization has also been reported in certain

composition range of Ga–Sb alloys that exhibit higher thermal stability than GST and sufficient optical and electrical contrasts.<sup>9–11</sup>

According to the Cu–Ge–Te ternary phase diagram reported by Dogguy et al.,<sup>12</sup> GCT compound is situated in the pseudobinary line between GeTe and CuTe binary compounds. GeTe compound is a promising PCM for PCRAM because of its better retention characteristic and larger electrical contrast between amorphous and crystalline phases than GST film.<sup>13,14</sup> GeTe amorphous film shows a volume shrinkage (–8%) and increment of reflectance upon crystallization, which are general features for PCMs.<sup>1,7</sup> These results suggest that there is a film composition showing nonvolume change and reflectance change upon crystallization on the pseudobinary line between GeTe and GCT compounds. Generally, repetitive change in volume results in an accumulation of stress at the interfaces between phase change material and surrounding materials such as electrodes and insulators. Such stress should cause void formation or delamination and finally breakdown of the cell.<sup>15–17</sup> Therefore, a small volume difference between amorphous and crystalline states is required in terms of the cyclability of PCRAM.<sup>18</sup>

Received: July 3, 2014

Revised: October 3, 2014

Published: October 22, 2014

In this paper, we investigated the compositional dependences of the phase change characteristics, such as crystallization temperatures, film thickness and reflectance changes upon crystallization, and crystallization starting time of the films on the GeTe–GCT–CuTe compositional line.

## EXPERIMENTAL SECTION

The approximately 200 nm thick Ge–Cu–Te amorphous films with the composition on the GeTe–CuTe pseudobinary line, including  $\text{GeCu}_2\text{Te}_3$ , were deposited on  $\text{SiO}_2(20\text{ nm})/\text{Si}(0.7\text{ mm})$  substrates at room temperature by RF cosputtering of GeTe (Ge 99.99%, Te 99.99%) and CuTe (Cu 99.9%, Te 99.99%) alloy targets. Sample compositions were controlled by adjusting the sputter power ratio of the GeTe and CuTe targets and were measured by scanning electron microscopy with energy dispersive spectroscopy (SEM-EDS), where the chemical composition was calibrated by the quantitative results obtained with inductively coupled plasma mass spectrometry (ICP-MS). The composition was measured in the as-deposited amorphous samples. The compositions of obtained samples were plotted on the Cu–Ge–Te ternary phase diagram in Figure 1. It can be seen that the chemical compositions of

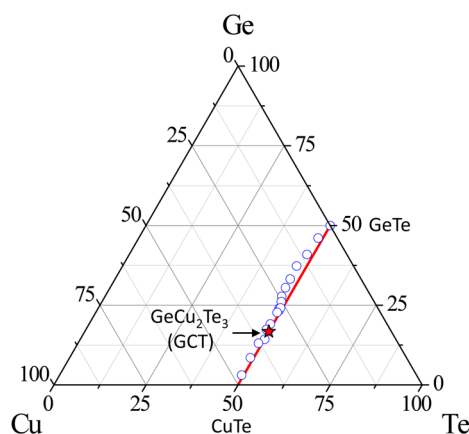


**Figure 1.** Composition diagram of prepared films. The obtained films exist along with the GeTe and CuTe pseudobinary line including  $\text{GeCu}_2\text{Te}_3$  (GCT).

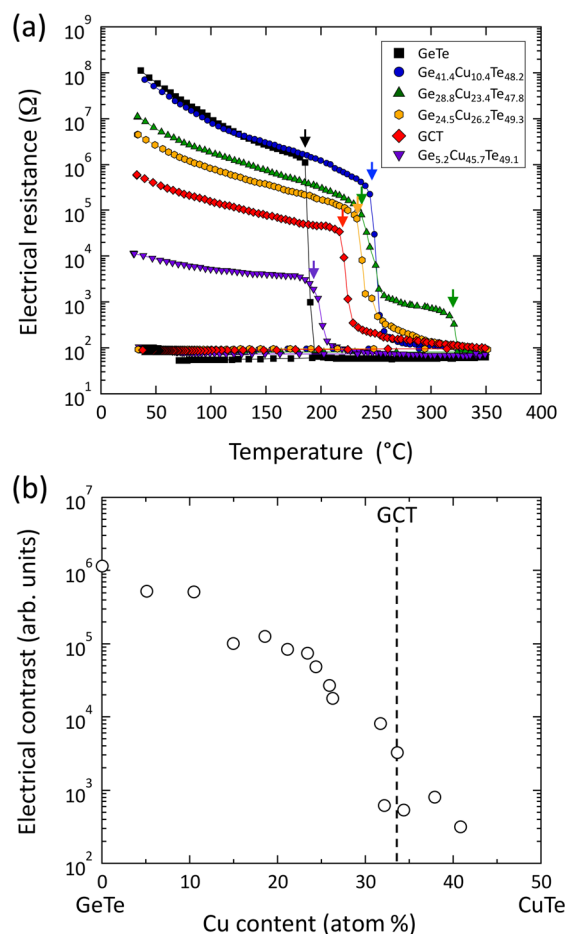
obtained samples almost entirely lie on the GeTe–CuTe pseudobinary line, which indicates that the composition of the obtained films can be almost expressed as  $\text{Ge}_{50-x}\text{Cu}_x\text{Te}_{50}$ . In this study, in order to focus on the Cu content, the obtained films were designated using Cu content, such as 10.4Cu film for  $\text{Ge}_{41.4}\text{Cu}_{10.4}\text{Te}_{48.2}$ . Moreover, since the  $\text{Ge}_{17.4}\text{Cu}_{33.6}\text{Te}_{49.0}$  sample had the composition closest to stoichiometric  $\text{GeCu}_2\text{Te}_3$  ( $\text{Ge}_{16.7}\text{Cu}_{33.3}\text{Te}_{50.0}$ ) and a compositional deviation of max 1 atom % for all elements, this sample was designated as GCT. It was confirmed from X-ray diffraction (XRD) analysis that all as-deposited films were in amorphous states with a broad peak, where XRD was carried out with  $\theta/2\theta$  scan mode using  $\text{Cu K}\alpha$  (wavelength:  $1.541\text{ \AA}$ ) as an X-ray source. The as-deposited films were heated to  $350\text{ }^\circ\text{C}$  at a heating rate of  $10\text{ }^\circ\text{C}/\text{min}$  in an Ar atmosphere to prepare the crystalline films and then cooled to room temperature. The resistance changes were measured during heating and cooling by the two-point probe method. XRD analyses were carried out for annealed samples to investigate the phase change behavior. The thicknesses of the as-deposited amorphous and the annealed crystalline  $\text{Ge}_{50-x}\text{Cu}_x\text{Te}_{50}$  films were measured with atomic

force microscopy (AFM) to examine volume change associated with the crystallization. For AFM measurements, a part of the substrate surface was covered with a marker before the deposition. After deposition, the marker was removed by ethanol to create a step. And then the thickness of the film was measured before and after annealing. The scan length was  $200\text{ }\mu\text{m}$ , which was long enough to measure the film thickness precisely. The experimental error of this method was less than  $\pm 2.5\%$  for both amorphous and crystalline films, and the subsequent error on the film thickness change was approximately less than  $\pm 3.5\%$ , where the root-mean-square roughness in the film surface was less than  $2\text{ nm}$  in both of the as-deposited and annealed films. The relative reflectance was measured with a spectrophotometer for amorphous and crystalline films in the wavelength range between  $400$  and  $1000\text{ nm}$  with respect to the reflectance of an Al reference mirror. In order to evaluate the crystallization time, the reflectance was measured with a static laser tester operated at constant laser power and pulse width. A pump pulse laser was used to provide thermal energy for crystallization, while a probe pulse laser was used to measure reflectance. Both pump pulse and probe pulse laser beams were operated at a constant wavelength of  $830\text{ nm}$ . Obtained results were analyzed to reveal crystallization behavior with special attention to the crystallization starting time ( $t_c$ ) of the as-deposited amorphous films.

## RESULTS AND DISCUSSION

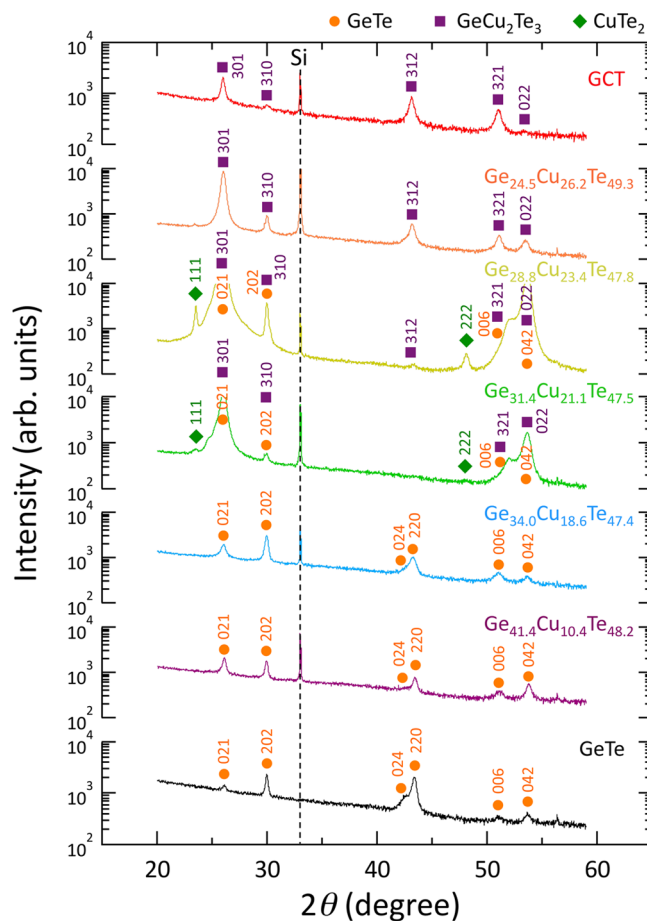
**1. Electrical and Structural Transition.** Figure 2a shows the temperature dependence of electrical resistance of six samples measured at a constant heating rate of  $10\text{ }^\circ\text{C}/\text{min}$ , where as-deposited films were confirmed to be in an amorphous state by XRD measurements. The electrical resistance of the films decreases with increasing heating temperature. When the temperature reaches the crystallization temperature,  $T_x$  of each film, a sudden drop of electrical resistance is seen, as shown by arrows in Figure 2a. The  $T_x$  of the amorphous GeTe film is about  $188\text{ }^\circ\text{C}$ , which is in good agreement with the reported value.<sup>13</sup> It is seen that the 23.4 atom % Cu film shows a two-step resistance drop. Such a two-step resistance drop was observed in the film with a composition range of  $21.1\text{ atom \%} \leq \text{Cu} \leq 24.3\text{ atom \%}$ , resulting from the two-stage crystallization process, as mentioned later. It is seen that the electrical resistance of the amorphous state of the films decreases with increasing Cu content, while that of the crystalline state is almost constant, independent of the film composition. Consequently, the electrical contrast between the amorphous and crystalline states decreases with increasing Cu content, as shown in Figure 2b, where the electrical contrast was calculated by dividing the resistance of the amorphous phase at  $50\text{ }^\circ\text{C}$  by that of the crystalline phase at  $50\text{ }^\circ\text{C}$ .

Figure 3 shows the XRD patterns of GeTe, 10.4Cu, 18.6Cu, 21.1Cu, 23.4Cu, 26.2Cu, and GCT films after heating to  $350\text{ }^\circ\text{C}$  followed by cooling to room temperature. The GeTe film crystallizes to a rhombohedral structure, which can be viewed as a distorted NaCl-type structure.<sup>19,20</sup> Until the Cu content up to 18.6 atom %, the XRD peaks of films are very similar to that of GeTe film and consequently, can be identified as a rhombohedral-GeTe structure and no other peaks were observed. The XRD patterns of the 21.1Cu and 23.4Cu films showing a two-step resistance drop drastically changes and the intensities of the peaks at around  $26.0^\circ$  and  $53.6^\circ$  become much higher. In addition, new small peaks appear at around  $23.5^\circ$  and



**Figure 2.** (a) Temperature dependence of electrical resistance of the GeTe (205.5 nm), 10.4Cu (197.2 nm), 23.4Cu (199.7 nm), 26.2Cu (202.0 nm), GCT (198.1 nm), and 45.7Cu (190.8 nm) films, where the value in parentheses indicates the film thicknesses in their as-deposited state. (b) Compositional dependence of electrical contrast between amorphous and crystalline phases measured at 50 °C.

48.1°. Those results indicate that the 21.1Cu and 23.4Cu crystallize to GCT and GeTe mixed-phase with a small amount of CuTe<sub>2</sub> phase. Moreover, it was confirmed by XRD measurements that the first resistance drop corresponds to the crystallization to the GCT phase with a small amount of CuTe<sub>2</sub> crystalline phase. It was also confirmed by transmission electron microscopy (TEM) observation (not shown) that the amorphous phase still remains after the first resistance drop. And the second drop was due to the crystallization of the residual amorphous phase to GeTe. Meanwhile, in the XRD patterns of the 26.2Cu and GCT films, only a peak at around 26.0° shows a higher intensity and consequently, those films are suggested to crystallize to a GeCu<sub>2</sub>Te<sub>3</sub> single-phase.<sup>21</sup> Here, since the XRD peak positions of GeCu<sub>2</sub>Te<sub>3</sub> are very similar to those of rhombohedral GeTe, it is difficult to distinguish whether the GCT film is a GeCu<sub>2</sub>Te<sub>3</sub> single-phase or a GeCu<sub>2</sub>Te<sub>3</sub> + GeTe two-phase only from the XRD peak positions. However, the relative intensities of the XRD patterns of GeCu<sub>2</sub>Te<sub>3</sub> are clearly different with those of GeTe. GeTe has the highest peak at around 29.8° and the second one at around 43.3°, while GeCu<sub>2</sub>Te<sub>3</sub> has the highest peak at around 25.9° and the second one at around 43.0° in the XRD patterns. The relative intensities of the obtained XRD pattern in the GCT film is correspond to those of the powder reference pattern of



**Figure 3.** XRD patterns of the GeTe, 10.4Cu, 18.6Cu, 21.1Cu, 23.4Cu, 26.2Cu, and GCT films measured at room temperature after heating to 350 °C.

GeCu<sub>2</sub>Te<sub>3</sub>. Moreover, it was confirmed by ICP-MS measurement that the composition of the GCT film was Ge<sub>17.4</sub>Cu<sub>33.6</sub>Te<sub>49.0</sub> and the deviation from the stoichiometric composition of GeCu<sub>2</sub>Te<sub>3</sub> was found to be max 4% for every element. Based on the above discussion, the GCT film should show the crystallization into a GeCu<sub>2</sub>Te<sub>3</sub> single-phase without phase separation upon crystallization.

Figure 4 shows the compositional dependence of the  $T_x$  and summarizes the crystalline phases after crystallization obtained from XRD and TEM results in each composition range. The  $T_x$  was obtained by finding the minimum value of the first derivative of the electrical resistance with temperature. As shown in Figure 4, the  $T_x$  increases with increasing Cu content and reaches a maximum of about 250 °C at around 15 atom % Cu and then decreases with further increasing Cu content. This result suggests that Cu is effective to increase the crystallization temperature of GeTe film.

It was found that the crystalline state with a rhombohedral-GeTe structure can be obtained in film with a Cu content of below 18.6 atom %, although it has been reported that Cu cannot be dissolved into the GeTe phase in a thermodynamic equilibrium state.<sup>12</sup> Generally, it is known that a metastable supersaturated phase can be obtained in nanoscale material such as thin film. The present results indicate that Cu may be metastably soluble up to about 19 atom % in GeTe. In addition, Sun et al. have pointed out from ab initio calculations<sup>22</sup> that doped Cu atoms can occupy vacancies at Ge sites in a



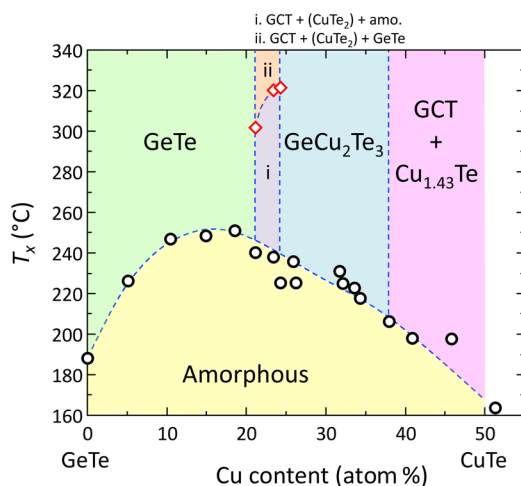


**Figure 4.** Compositional dependence of  $T_x$  and detected crystalline phases after crystallization, where the  $T_x$  was determined by resistance measurement.

rhombohedral-GeTe structure.<sup>23</sup> It has also been found that film crystallizing to a  $\text{GeCu}_2\text{Te}_3$  phase can be obtained in a wide composition range of  $26.2 \text{ atom } \% \leq \text{Cu} \leq 37.9 \text{ atom } \%$ , although the  $\text{GeCu}_2\text{Te}_3$  phase is a line compound in the equilibrium state.<sup>12</sup> The films with an intermediate composition in between those of the films showing the crystallization to GeTe and  $\text{GeCu}_2\text{Te}_3$  single-phase show a two-step crystallization and finally form a GeTe and GCT mixed-phase with a small amount of the  $\text{CuTe}_2$  phase. The formation of a small amount of the  $\text{CuTe}_2$  phase is thought to be caused by a small composition deviation from the GeTe–CuTe pseudobinary line, as shown in Figure 1. Meanwhile, it was found from XRD analyses (not shown) that the film with a Cu content of over 38 atom % showed a simultaneous crystallization to GCT and  $\text{Cu}_{1.43}\text{Te}$  phases.

**2. Thickness Change upon Crystallization.** In this study, the volume change was evaluated by measuring the thickness change of the film upon crystallization. Thickness was determined by AFM measurements at room temperature before and after crystallization (heated to  $350^\circ\text{C}$ ), and thickness change,  $\Delta t/t$ , was defined as  $(t_{\text{cry}} - t_{\text{amo}})/t_{\text{amo}} \times 100$  (%), where  $t_{\text{cry}}$  and  $t_{\text{amo}}$  are the thickness of the film in the crystalline and amorphous state, respectively. Figure 5a shows the compositional dependence of the thickness change upon crystallization. The GeTe film shows the decrease in thickness of about 7.8% upon crystallization, which is similar to that of other reported PCMs ( $\text{Ge}_2\text{Sb}_{2.04}\text{Te}_{4.74}$  (hexagonal), 8.2% (thickness change);<sup>24</sup>  $\text{Ge}_{14.5}\text{Sb}_{85.5}$ , 8% (density change)<sup>25</sup>). The reduction in thickness upon crystallization decreases with increasing Cu content, and the film with about 23 atom % Cu shows almost no change in thickness upon crystallization, which means almost no volume change upon phase change. The films with over 25 atom % Cu show an increase in film thickness upon crystallization, and the GCT film shows an increase in thickness of about 3.4%. Since the film with Cu content of above 38 atom % showed a rough surface in the crystalline state and, consequently, the obtained data were considerably scattered, the data could not be plotted in Figure 5a. This was thought to be due to the formation of the  $\text{Cu}_{1.43}\text{Te}$  phase, which was confirmed by XRD measurements.

Based on the dependence of Cu content on crystallization process, the thickness change plots are divided into three

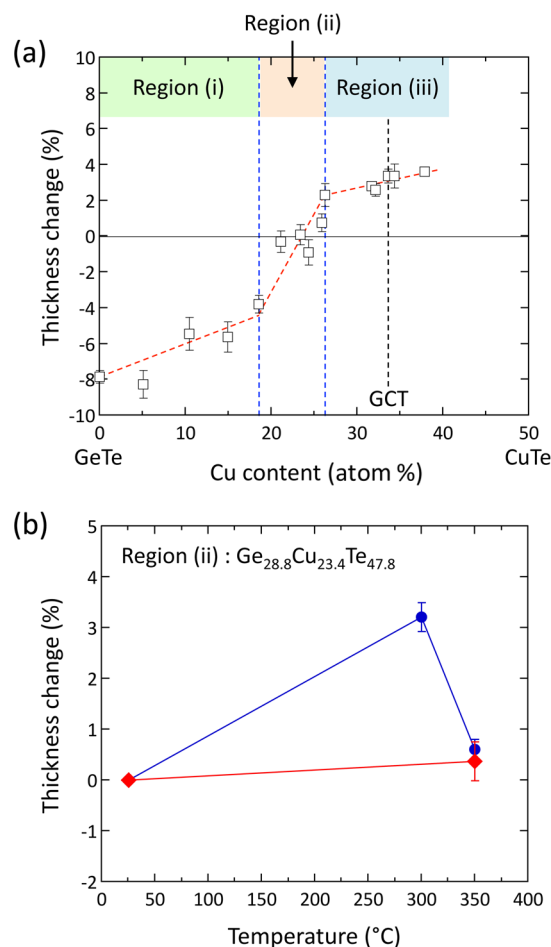


**Figure 5.** (a) Compositional dependence of the film thickness change on crystallization. (b) Heating temperature dependence of the film thickness change of 23.4Cu film.

regions (i, ii, and iii) depending on the Cu content. It is seen that there are almost linear relationships between thickness change and Cu content in each region. In regions (i) and (iii), the films show crystallization into the GeTe phase and the GCT phase, respectively. It is noteworthy that the 26.2Cu film shows only about a 2% increase in film thickness upon crystallization without phase separation. Meanwhile, in region (ii), the films show two-stage crystallization. The slope of the plots in region (ii) is larger than those in regions (i) and (iii). When two phases coexist, it can be said that the thickness change is dominated by the volume ratio of each phase.

Here, we discuss the relative absence of thickness change upon crystallization obtained in the 23.4Cu film exhibiting two-stage crystallization, as shown in Figure 2a. Figure 5b exhibits the thickness change as a function of heating temperature of the 23.4Cu film. When this film was directly heated to  $350^\circ\text{C}$  and then cooled to room temperature, the thickness change was small, that is, less than 0.5%. However, a thickness increase of about 3.2% was observed when the film was heated to  $300^\circ\text{C}$  and then cooled to room temperature, indicating that the first resistance drop corresponds to crystallization to the GCT phase with a small amount of Cu–Te binary phase, which also shows a volume expansion upon crystallization. It is noteworthy that after heating this film again to  $350^\circ\text{C}$  followed by cooling, it shows a decrease in thickness again, and the total thickness change is about +0.6%. These results support the idea that the

second resistance drop is mainly due to the crystallization of residual amorphous phase to GeTe, accompanied by a reduction of thickness. It can be suggested that the relative absence of volume change was achieved in the 23.4Cu film by two-step crystallization of GCT (volume expansion) and GeTe (volume shrinkage).

**3. Relative Reflectance Measurements.** The results of relative reflectance measurements in amorphous and crystalline states are shown in Figure 6a and b, respectively, for films with

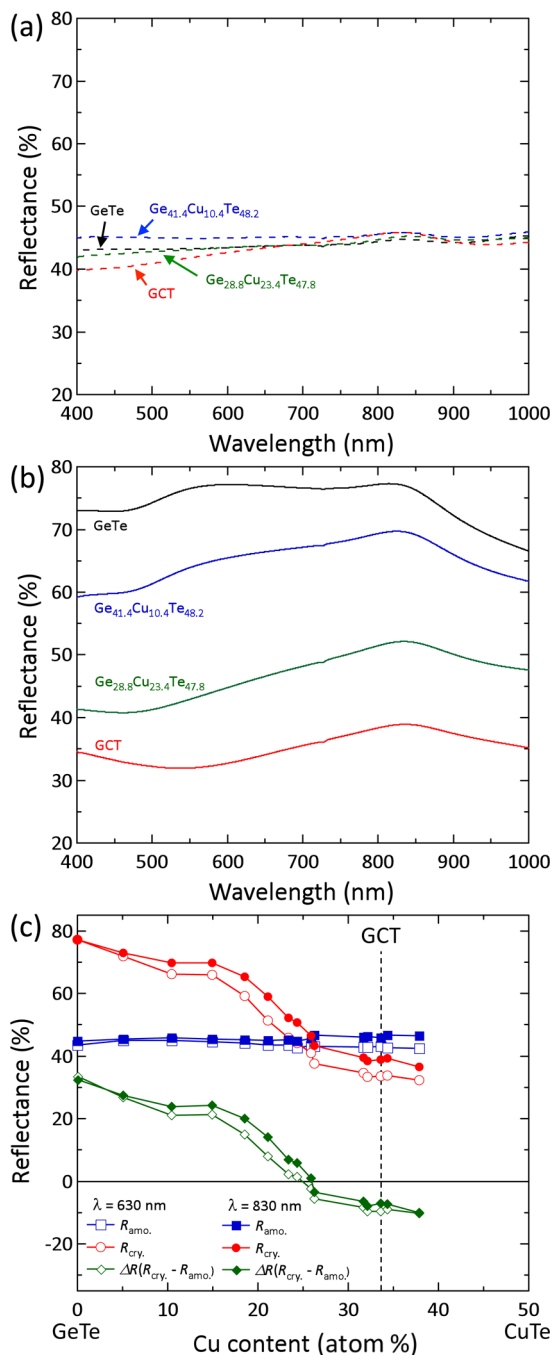


**Figure 6.** Wavelength dependence of reflectance of the GeTe, 10.4Cu, 23.4Cu, and GCT films in (a) as-deposited amorphous and (b) 350 °C annealed crystalline states, respectively. (c) Compositional dependence on  $R_{\text{amo}}$  and  $R_{\text{cry}}$  at the wavelengths of 630 and 830 nm. The differences of the reflectance ( $\Delta R = R_{\text{cry}} - R_{\text{amo}}$ ) are also plotted.

Cu content of 0, 10.4, 23.4, and 33.6 (GCT), where the crystalline state was obtained by heating up to 350 °C followed by cooling. The results of the film with Cu content of over 40.8 atom % were omitted because the film showed a large surface roughness after crystallization. It is seen that the reflectance of the amorphous phase does not show a significant compositional dependence and exhibits around 45% in this wavelength range. On the other hand, the reflectance of the crystalline phase has a large compositional dependence and Cu-rich films, including GCT, show a decrease in reflectance upon crystallization. Recently, several phase change materials have been reported to show inverse mass density change and reflectance change.<sup>7,8,10,11,25,26</sup> The compositional dependences of reflectance in amorphous and crystalline states are shown in Figure 6c measured at wavelengths of 630 and 830 nm. This wavelength is important for application to optical discs<sup>27</sup> and is used for the evaluation of crystallization speed in this study, as mentioned later, respectively. The  $R_{\text{amo}}$  is almost independent of the sample composition in both wavelengths, while the  $R_{\text{cry}}$  monotonically decreases with increasing Cu content. It is seen that there is a film composition showing almost no reflectance change between amorphous and crystalline states. Figure 7 presents plots of the reflectance

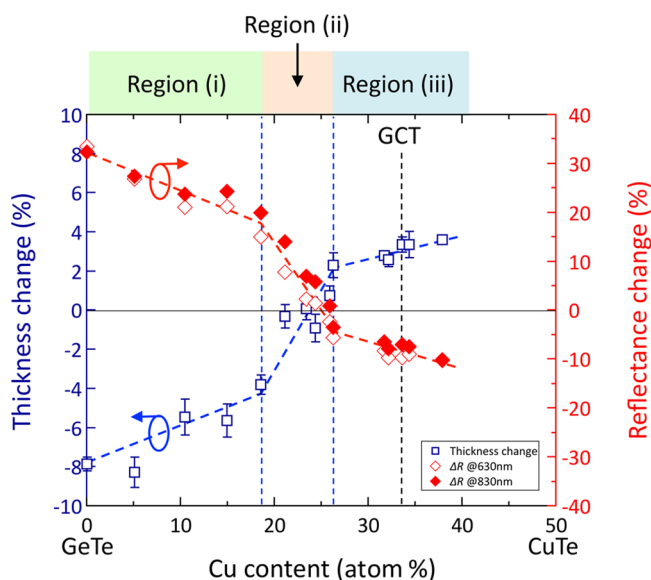


**Figure 7.** Compositional dependence of the film thickness change and the reflectance change.

change,  $\Delta R$  ( $\Delta R = R_{\text{cry}} - R_{\text{amo}}$ ), upon crystallization as a function of Cu content at wavelengths of 630 and 830 nm together with the results of thickness change. The plots are divided into three regions as are the thickness change plots depending on phase constitution. It is noteworthy that the film composition showing nonreflectance change upon crystallization is almost the same as that showing nonvolume change upon crystallization, which means that there is a correlation between thickness change (density change) and reflectance change upon crystallization.

**4. Relationship between Thickness Change and Reflectance Change.** Detemple et al. have reported that there is a clear correlation between optical contrast and density change upon crystallization for PCMs.<sup>27</sup> Recently, the present authors have reported that an approximately linear relationship was obtained between the optical contrast and the density

change in many PCMs and that this can be extended to the negative region including in GCT film.<sup>7</sup> Figure 8 shows the

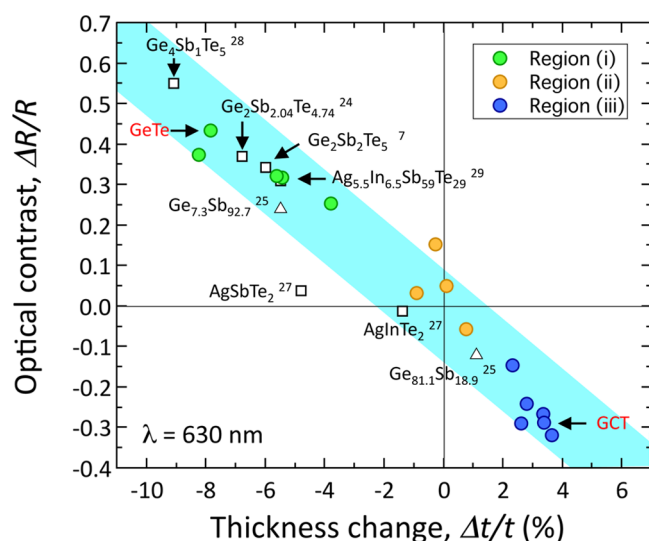


**Figure 8.** Relationship between optical contrast and thickness change for various phase change materials. Filled circles are the data of  $\text{Ge}_{50-x}\text{Cu}_x\text{Te}_{50}$  alloy films obtained in this study. Squares and triangles are the data of thickness change from refs 7, 24, and 27–29, and density change from ref 25.

plots of optical contrast versus thickness change for various PCMs, including the data of the film obtained in this study.<sup>7,24,25,27–29</sup> The optical contrast,  $\Delta R/R$ , was defined as  $(R_{\text{cry}} - R_{\text{amo}})/R_{\text{cry}}$  using the values of relative reflectance,  $R$ , of the film. Here, since it has been reported that the density change showed in good agreement with the thickness change in the crystallization process of phase change materials,<sup>24,29</sup> the values of the density change for the Ge–Sb alloys<sup>25</sup> were also plotted in Figure 8. It is seen from Figure 8 that the  $\text{Ge}_{50-x}\text{Cu}_x\text{Te}_{50}$  films also satisfy the approximately linear relationship between optical contrast and thickness change even if the films have a mixture-phase, and the PCMs with almost no optical contrast seem to show almost no change in thickness. A large optical contrast is important for optical discs to ensure precise reading, while a large electrical contrast is more important for PCRAM application, while a large density change would be a problem for PCRAM because it can lead to void formation and, consequently, degrade the cyclic ability.<sup>15–17,25</sup> The ideal PCMs for PCRAM application are expected to show a large electrical contrast and no change in volume upon crystallization. In other words, it is suggested from Figure 8 that a PCM, which shows a small optical contrast without loss of the electrical contrast, is suitable for PCRAM application with regard to the cyclability. Further work on the cyclability of PCRAM using phase change materials showing a small volume change upon crystallization are needed.

**5. Crystallization Speed.** Figure 9a shows the normalized reflectance,  $R/R_0$ , as a function of the pulse width of a pump laser at a constant power of 5.7 mW for four kinds of film: 0Cu, 10.4Cu, 23.4Cu, and GCT. Here, the reflectance is measured using voltages detected by a photodiode before ( $R_0$ ) and after ( $R$ ) pump laser irradiation. It is seen from Figure 9a that the binary GeTe and 10.4Cu films show drastic increases in reflectance. On the other hand, the 23.4Cu and GCT films do not show such an increase in reflectance and data scatter at

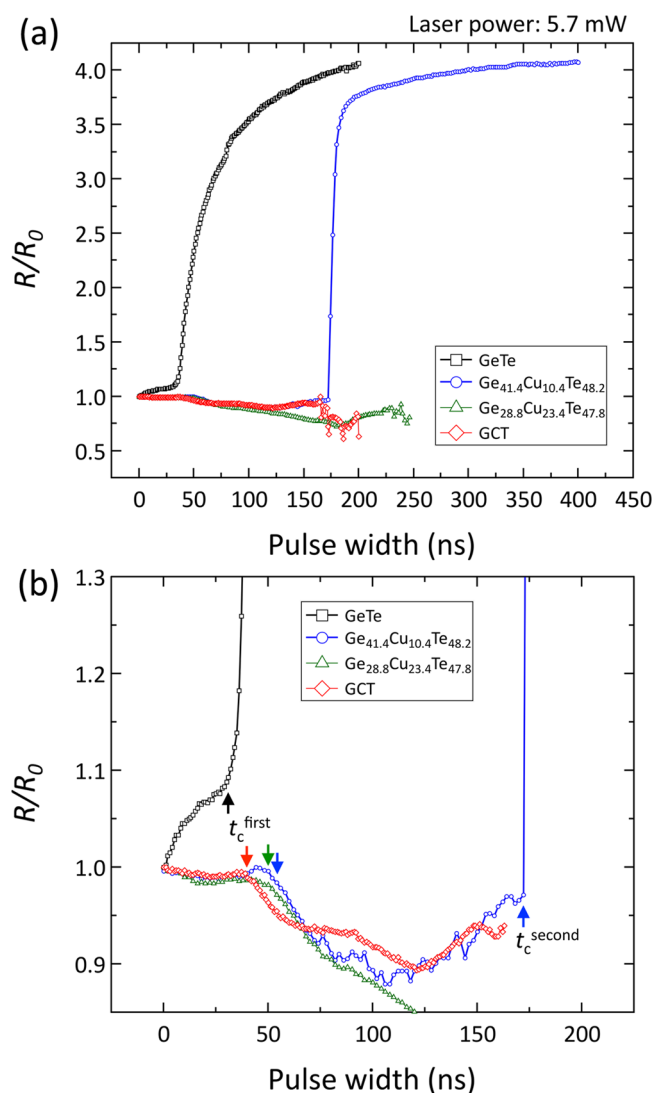


**Figure 9.** (a) Normalized reflectance changes as a function of pulse width of the GeTe, 10.4Cu, 23.4Cu, and GCT films at a laser power of 5.7 mW. (b) Magnified image of (a) focusing on the crystallization starting time.

longer pulse duration. The data scattering is due to ablation of the film.<sup>7</sup> Figure 9b indicates the magnified area of Figure 9a to focus on the onset of crystallization. The gradual increase of reflectance in the amorphous GeTe before the onset of crystallization might be due to the structural relaxation of amorphous film.<sup>30,31</sup> As shown in Figure 9b, a small reflectance decrease is observed at around 50 ns except in the binary GeTe film. The arrows in Figure 9b indicate the crystallization starting time ( $t_c$ ) for each sample. Since the GCT film shows negative change in reflectance upon crystallization, as shown in Figure 6, the decrease in the reflectance observed in Figure 9b is thought to be due to the formation of the crystalline  $\text{GeCu}_2\text{Te}_3$  phase. Interestingly, the 10.4Cu film shows two-step reflectance change. Judging from the sign of the reflectance change, the first decrease in reflectance at around 50 ns corresponds to the crystallization to  $\text{GeCu}_2\text{Te}_3$  and the second increase in reflectance at 175 ns corresponds to the formation of GeTe.

The compositional dependence of  $t_c$  is shown in Figure 10a. The films with Cu content of 0–5.1 atom % and of above 21.1

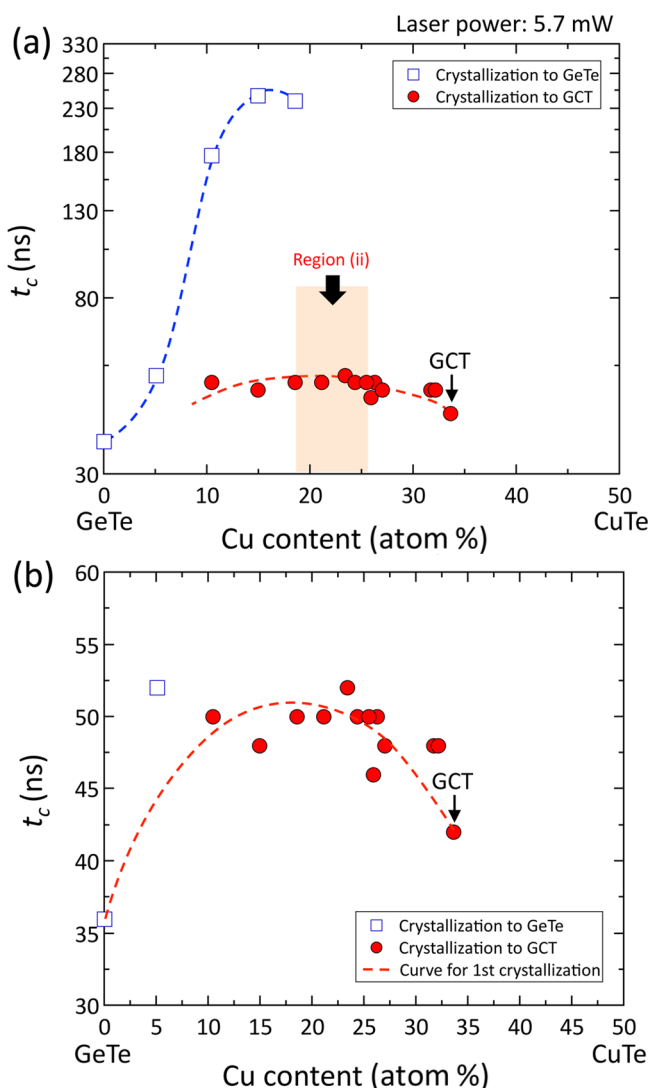


**Figure 10.** (a) Compositional dependence of the crystallization starting time. (b) Compositional dependence of the first crystallization time.

atom % show a single change in reflectance corresponding to the crystallization to the GeTe and  $\text{GeCu}_2\text{Te}_3$  phases, respectively, while the films with Cu content of 10.5–18.6 atom % show a two-step reflectance change. It is noted that the composition range showing two-step phase change is different between laser irradiation measurement and in situ resistance measurement. This difference may be due to the difference of heating rate for crystallization. In situ resistance measurements were carried out at a heating rate of  $10\text{ }^\circ\text{C}/\text{min}$  on a hot plate, while laser irradiation measurements were carried out with a nanosecond-order pulse width to heat up the film. Such a large difference in heating time and heating method must affect the crystallization behavior of amorphous film. Especially, in the nonstoichiometric composition film showing phase separation, the crystallization behavior is suggested to be more sensitive to heating conditions. Ortiz et al. reported that rapid laser heating of the amorphous phase might produce a metastable phase not obtainable by conventional annealing.<sup>30</sup> Further work is needed to understand the crystallization mechanism of rapid laser heated amorphous  $\text{Ge}_{50-x}\text{Cu}_x\text{Te}_{50}$  films. Figure 10b shows the magnified area of Figure 10a to focus on the first crystallization

starting time,  $t_c^{\text{first}}$ . It is seen that the  $t_c^{\text{first}}$  becomes smaller as the composition becomes closer to stoichiometric, namely, GeTe and  $\text{GeCu}_2\text{Te}_3$  compounds. This trend is similar to the results of the compositional dependence on crystallization time of the Ge–Te binary system.<sup>32,33</sup> In the Ge–Te binary system, stoichiometric GeTe has the shortest crystallization time and once the composition of the film deviates from stoichiometry to Ge-rich or Te-rich composition, the crystallization time significantly increases because of the necessity of long-range diffusion of the atoms during crystallization. Nonstoichiometric Ge–Te films show 10 to more than 100 times slower crystallization time than stoichiometric GeTe compound;<sup>32,33</sup> however,  $\text{Ge}_{50-x}\text{Cu}_x\text{Te}_{50}$  films do not show such an extreme large difference in the crystallization time between stoichiometric and nonstoichiometric composition films. This should be preferable for PCRAM application, because the present pseudobinary alloy film is relatively robust against a compositional deviation.

## CONCLUSIONS

In this study, phase change characteristics of GeTe–CuTe pseudobinary alloy film including  $\text{GeCu}_2\text{Te}_3$  (GCT) were investigated. The crystallization temperature increased with increasing Cu content, and after it reached the maximum at around 15 atom % Cu, it decreased again with increasing Cu content. The crystallization process differed depending on the composition of the film. XRD results indicated that, in the composition range from 0 to 18.6 atom % Cu, the amorphous film crystallized to a GeTe phase, and similarly, to a  $\text{GeCu}_2\text{Te}_3$  phase in the composition range from 26.2 to 37.9 atom % Cu. On the other hand, the film of the composition range between 21.1 and 24.3 atom % Cu showed clear two-step crystallization during heating and finally formed a mixed phase of GeTe and  $\text{GeCu}_2\text{Te}_3$ .

The amount of shrinkage in film thickness upon crystallization decreased with increasing Cu contents and the film with around 23 atom % Cu showed almost no volume change upon crystallization. Meanwhile, the films with a composition of over 25 atom % Cu showed expansion in film thickness upon crystallization and the GCT film showed an expansion of about 3.4% in film thickness. It was found that almost nonvolume change was achieved by two-step crystallization, namely, first crystallization to  $\text{GeCu}_2\text{Te}_3$  (volume expansion) and second to GeTe (volume shrinkage).

The optical reflectance of amorphous  $\text{Ge}_{50-x}\text{Cu}_x\text{Te}_{50}$  film in the visible light range showed negligible compositional dependence, whereas that of crystalline film decreased monotonically with increasing Cu content. The films of the composition with no volume change between amorphous and crystalline phases showed no reflectance change upon crystallization.

The crystallization time of amorphous  $\text{Ge}_{50-x}\text{Cu}_x\text{Te}_{50}$  film showed only small dependence on the film composition. From the obtained results, it is suggested that nonstoichiometric  $\text{Ge}_{50-x}\text{Cu}_x\text{Te}_{50}$  films such as 26.2Cu film showing a small volume change without phase separation are preferable in terms of cyclability of PCRAM.

## AUTHOR INFORMATION

### Corresponding Authors

\*Tel: +81-29-861-8013. Fax: +81-29-851-2902. E-mail: yuta-saito@aist.go.jp.



\*Tel: +81-22-795-7338. Fax: +81-22-795-7338. E-mail: ysutou@material.tohoku.ac.jp.

## Notes

The authors declare no competing financial interest.

## ACKNOWLEDGMENTS

This work was supported by KAKENHI (23360297), and partially supported by a Grant-in-Aid for JSPS fellows from the Ministry of Education, Culture, Sports, Science and Technology, Japan (10J05810).

## REFERENCES

- (1) Wuttig, M.; Yamada, N. Phase-Change Materials for Rewriteable Data Storage. *Nat. Mater.* **2007**, *6*, 824–832.
- (2) Yamada, N.; Ohno, E.; Nishiuchi, K.; Akahira, N.; Takao, M. Rapid-Phase Transitions of GeTe-Sb<sub>2</sub>Te<sub>3</sub> Pseudobinary Amorphous Thin Films for an Optical Disk Memory. *J. Appl. Phys.* **1991**, *69*, 2849–2856.
- (3) Lai, S.; Lowrey, T. OUM - A 180 nm Nonvolatile Memory Cell Element Technology for Stand Alone and Embedded Applications. *Technol. Dig. - Int. Electron Devices Meet.* **2001**, 36.5.1–36.5.4.
- (4) Sutou, Y.; Kamada, T.; Sumiya, M.; Saito, Y.; Koike, J. Crystallization Process and Thermal Stability of Ge<sub>1</sub>Cu<sub>2</sub>Te<sub>3</sub> Amorphous Thin Films for Use as Phase Change Materials. *Acta Mater.* **2012**, *60*, 872–880.
- (5) Jovári, P.; Sutou, Y.; Kaban, I.; Saito, Y.; Koike, J. Fourfold Coordinated Te Atoms in Amorphous GeCu<sub>2</sub>Te<sub>3</sub> Phase Change Material. *Scr. Mater.* **2013**, *68*, 122–125.
- (6) Kamada, T.; Sutou, Y.; Sumiya, M.; Saito, Y.; Koike, J. Crystallization and Electrical Characteristics of Ge<sub>1</sub>Cu<sub>2</sub>Te<sub>3</sub> Films for Phase Change Random Access Memory. *Thin Solid Films* **2012**, *520*, 4389–4393.
- (7) Saito, Y.; Sutou, Y.; Koike, J. Optical Contrast and Laser-Induced Phase Transition in GeCu<sub>2</sub>Te<sub>3</sub> Thin Film. *Appl. Phys. Lett.* **2013**, *102*, 051910-1–051910-5.
- (8) Skelton, J. M.; Kobayashi, K.; Sutou, Y.; Elliott, S. R. Origin of the Unusual Reflectance and Density Contrasts in the Phase-Change Material Cu<sub>2</sub>GeTe<sub>3</sub>. *Appl. Phys. Lett.* **2013**, *102*, 224105-1–224105-4.
- (9) Raoux, S.; König, A. K.; Cheng, H.-Y.; Garbin, D.; Cheek, R. W.; Jordan-Sweet, J. L.; Wuttig, M. Phase Transitions in Ge-Sb Phase Change Alloys. *Phys. Status Solidi B* **2012**, *249*, 1999–2004.
- (10) Putero, M.; Coulet, M.-V.; Ouled-Khachroum, T.; Muller, C.; Baecht, C.; Raoux, S. Phase Transition in Stoichiometric GaSb Thin Films: Anomalous Density Change and Phase Segregation. *Appl. Phys. Lett.* **2013**, *103*, 231912-1–231912-5.
- (11) Putero, M.; Coulet, M.-V.; Ouled-Khachroum, T.; Muller, C.; Baecht, C.; Raoux, S. Unusual Crystallization Behavior in Ga-Sb Phase Change Alloys. *APL Mater.* **2013**, *1*, 062101-1–062101-7.
- (12) Dogguy, M.; Carcaly, C.; Rivet, J.; Flahaut, J. Description du Systeme Ternaire Cu-Ge-Te. *J. Less-Common Met.* **1977**, *51*, 181–199.
- (13) Fantini, A.; Perniola, L.; Armand, M.; Nodin, J. F.; Sousa, V.; Persico, A.; Cluzel, J.; Jahan, C.; Maitrejean, S.; Lhostis, S.; et al. Comparative Assessment of GST and GeTe Materials For Application to Embedded Phase-Change Memory Devices. *IEEE Int. Memory Workshop (Monterey)* **2009**, 1–2.
- (14) Perniola, L.; Sousa, V.; Fantini, A.; Arbaoui, E.; Bastard, A.; Armand, M.; Fargeix, A.; Jahan, C.; Nodin, J.-F.; Persico, A.; et al. Electrical Behavior of Phase-Change Memory Cells Based on GeTe. *IEEE Electron Device Lett.* **2010**, *31*, 488–490.
- (15) Lacaita, A. L. Phase Change Memories: State-of-the-Art, Challenges and Perspectives. *Solid-State Electron.* **2006**, *50*, 24–31.
- (16) Do, K.; Lee, D.; Ko, D.-H.; Sohn, H.; Cho, M.-H. TEM Study on Volume Changes and Void Formation in Ge<sub>2</sub>Sb<sub>2</sub>Te<sub>3</sub> Films, with Repeated Phase Changes. *Electrochem. Solid-State Lett.* **2010**, *13*, H284–H286.
- (17) Shin, S.; Kim, K. M.; Song, J.; Kim, H. K.; Choi, D. J.; Cho, H. H. Thermal Stress Analysis of Ge<sub>1</sub>Sb<sub>4</sub>Te<sub>7</sub>-Based Phase-Change Memory Devices. *IEEE Trans. Electron Devices* **2011**, *58*, 782–791.
- (18) Yin, Y.; Zhang, H.; Hosaka, S.; Liu, Y.; Yu, Q. Volume-Change-Free GeTeN Films for High-Performance Phase-Change Memory. *J. Phys. D: Appl. Phys.* **2013**, *46*, S05311-1–S05311-5.
- (19) Chattopadhyay, T.; Boucherle, J. X.; Schnering, H. G. Neutron Diffraction Study on the Structural Phase Transition in GeTe. *J. Phys. C: Solid State Phys.* **1987**, *20*, 1431–1440.
- (20) Krbal, M.; Kolobov, A. V.; Fons, P.; Tominaga, J.; Elliot, S. R.; Hegedus, J.; Giussani, A.; Perumal, K.; Calarco, R.; Matsunaga, T.; et al. Crystalline GeTe-Based Phase-Change Alloys: Disorder in Order. *Phys. Rev. B* **2012**, *86*, 045212-1–045212-6.
- (21) Delgado, G. R.; Mora, A. J.; Pirela, M.; Velásquez-Velásquez, A.; Villarreal, M.; Fernández, B. J. Structural Refinement of the Ternary Chalcogenide Compound Cu<sub>2</sub>GeTe<sub>3</sub> by X-ray Powder Diffraction. *Phys. Status Solidi A* **2004**, *201*, 2900–2904.
- (22) Sun, Z.; Tian, S.; Sa, B. Investigation of the Structure and Properties of Rhombohedral Cu-Ge-Te Alloys by Ab Initio Calculations. *Intermetallics* **2013**, *32*, 292–296.
- (23) Kolobov, A. V.; Tominaga, J.; Fons, P.; Uruga, T. Local Structure of Crystallized GeTe Films. *Appl. Phys. Lett.* **2003**, *82*, 382–384.
- (24) Njoroge, W. K.; Wöltgens, H.-W.; Wuttig, M. Density Changes upon Crystallization of Ge<sub>2</sub>Sb<sub>2.04</sub>Te<sub>4.74</sub> Films. *J. Vac. Sci. Technol., A* **2002**, *20*, 230–233.
- (25) Raoux, S.; Cabral, C., Jr.; Krusin-Elbaum, L.; Jordan-Sweet, J. L.; Virwani, K.; Hitzbleck, M.; Salinga, M.; Madan, A.; Pinto, T. L. Phase Transitions in Ge–Sb Phase Change Materials. *J. Appl. Phys.* **2009**, *105*, 064918-1–064918-8.
- (26) Fu, X. T.; Song, W. D.; Ho, H. W.; Ji, R.; Wang, L.; Hong, M. H. Anomalous Phase Change Characteristics in Fe-Te Materials. *Appl. Phys. Lett.* **2012**, *100*, 201906-1–201906-4.
- (27) Detemple, R.; Wamwangi, D.; Wuttig, M.; Bihlmayer, G. Identification of Te Alloys with Suitable Phase Change Characteristics. *Appl. Phys. Lett.* **2003**, *83*, 2572–2574.
- (28) Wamwangi, D.; Njoroge, W. K.; Wuttig, M. Crystallization Kinetics of Ge<sub>4</sub>Sb<sub>1</sub>Te<sub>5</sub> Films. *Thin Solid Films* **2002**, *408*, 310–315.
- (29) Njoroge, W. K.; Wuttig, M. Crystallization Kinetics of Sputter-Deposited Amorphous AgInSbTe Films. *J. Appl. Phys.* **2001**, *90*, 3816–3821.
- (30) Ortiz, C.; Blatter, A. Laser Irradiation of Amorphous Thin Films. *Thin Solid Films* **1992**, *213*, 209–218.
- (31) Coombs, J. H.; Jongenelis, A. P. J. M.; van Es-Spiekman, W.; Jacobs, B. A. Laser-Induced Crystallization Phenomena in GeTe-Based Alloys. I. Characterization of Nucleation and Growth. *J. Appl. Phys.* **1995**, *78*, 4906–4917.
- (32) Chen, M.; Rubin, K. A.; Barton, R. W. Compound Materials for Reversible, Phase-Change Optical Data Storage. *Appl. Phys. Lett.* **1986**, *49*, S02–S04.
- (33) Raoux, S.; Cheng, H.-Y.; Caldwell, M. A.; Wong, H.-S. P. Crystallization Times of Ge–Te Phase Change Materials as a Function of Composition. *Appl. Phys. Lett.* **2009**, *95*, 071910-1–071910-3.